Electronic Supplementary Material (ESI) for Journal of Materials Chemistry A.

Supplemental Information

A metal-ion-chelating organogel electrolyte for Le Chatelier depression of Mn^{3+} disproportionation of lithium manganese oxide spinel

Yoon-Gyo Cho, Seo Hyun Jung, Se Hun Joo, Yuju Jeon, Minsoo Kim, Kyung Min Lee, Seungmin Kim, Jong Mok Park, Hyun Kuk Noh, Young-Soo Kim, Jung-Eui Hong, Sang-Ik Jeon, Taewon Kim, Sang Kyu Kwak*, Hoyoul Kong* and Hyun-Kon Song*

Experimental

Pyrd-PVA-CN synthesis

PVA-CN (Shin-Etsu Chemical CRV) was used as the base polymer for making Pyrd-PVA-CN. 75.8 % of monomeric units of polyvinyl alcohol (PVA) was cyanoethylated according to the manufacturer's specification. Molecular weights were measured by gel permeation chromatography (GPC, Agilent technologies 1200 series). Poly(methyl methacrylate) (PMMA) standard was used with dimethylformamide (DMF) as an eluent at 30 ^{o}C in 1.00 mL min^{-1}. The number–average molecular weight (M_n) of PVA-CN was 109,300 g mol^{-1}. The number of alcoholic units (x mol) and the number of cyanoethyl units (y mol) were calculated by:

$$44\,x + 97\,y = 109{,}300 \qquad \text{and} \qquad y / (x+y) = 0.758$$

where the molecular weights of alcoholic units (vinyl alcohol) and cyanoethyl units (3-(vinyloxy)propanenitrile) are 44 g mol^{-1} and 97 g mol^{-1}, respectively. 314 alcoholic units and 984 cyanoethyl units were obtained as x and y, respectively (**Figure S7**).

Pyrd-PVA-CN was synthesized by functionalizing PVA-CN with pyrrolidone via esterification between an alcoholic group of PVA-CN and a carboxylic group of 2-pyrrolidone-5-carboxylic acid (PCA).[1] PVA-CN (7 g, 0.0385mol vinyl alcohol repeating unit), N,N'-Dicyclohexylcarbodiimide (DCC; 15.88 g, 0.077 mol) and PCA (9.94 g, 0.077 mol) were added sequentially into a 500 mL round-bottomed flask containing 175 mL dimethylformamide (DMF). The flask was immersed in an ice-water bath. 4-Dimethylaminopyridine (DMAP) (0.391 g) in 25 mL DMF was added to the mixture within 10 min. The reaction mixture was stirred for 40 h at room temperature, allowing insoluble DCC urea to precipitate out of solution. After filtration, the polymer product was precipitated in water to remove excess PCA. After re-dissolving the

product in DMF, polymer was precipitated again in ethanol to remove excess DCC urea and DCC. Finally, the product was dried under vacuum at 100 ^{o}C for 24 h. Pyrd-PVA-CN: M_n = 137,600 g mol^{-1}, M_w/M_n=1.72. ^{1}H NMR (300 MHz, DMSO-d_6. δ in ppm) (**Figure S6b**): 7.8 (1H, s, CH-NH-C=O), 5.03 (1H, s, CH_2-CH-O-(C=O)), 4.71 (1H, s, -O-(C=O)-CH), 4.38 (1H, s, CH_2-CH-OH), 3.63 (3H, s, O-CH_2-CH_2, CH_2-CH-OH), 2.71 (2H, s, CH_2-CH_2-CN), 2.25-1.2 (CH_2-CH-O-CH_2, -CH_2-CH-O-(C=O)-,CH_2-CH-OH). The NMR peak area of -NH was 61.5 % of the sum of the peak areas of -NH and –OH, indicating that the amide groups were about 1.6 times more than alcoholic groups. Based on the information, a strand of Pyrd-PVA-CN was estimated to be composed of 984 cyanoethyl units, 120 alcoholic units and 193 pyrrolidone units (**Figure S7**).

Active materials for cathodes and anodes

LMO (LG Chem.) was used as received for investigating its practical 4 V reaction. On the other hand, to investigate the 3 V reaction of LMO known to be unstable, graphene (Gn)-wrapped LMO nanoparticles (LMO@Gn) were synthesized. A mixture of LMO (Aldrich) and graphite (TIMCAL KS6) at 80 : 7 in weight was ball-milled in a stainless vial by using a high-energy vibratory ball miller (SPEX 8000D) for 6 h to produce LMO@Gn.

Cell preparation

The 2032 coin cells with a porous polyethylene separator (Asahi NH716) were used for all battery tests. Electrode compositions were described by weight. Cathode slurries were coated on aluminum foils, followed by drying at 100 ^{o}C under vacuum for 10 h. Anode slurries were coated on copper foils and then dried at 80 ^{o}C under vacuum.

Delithiation and lithiation of LMO spinel at ~4 V were electrochemically investigated in a half-cell configuration with lithium metal anode. **Cathode**: LMO: Super-P (TIMCAL): polyvinylidene fluoride (PVdF; Solvay) = 92 : 3 : 5. LMO loading = 17 mg cm^{-2}.

Delithiation and lithiation of LMO spinel at ~3 V were electrochemically investigated in a full-cell configuration with a prelithiated graphite anode. **Cathode**: LMO: Gn: PVdF: Super-P = 70 : 6.125 : 20 : 3.875; LMO@Gn loading = 0.7 mg cm^{-2}. **Anode**: prelithiated natural graphite (Mitsubishi Chemical): PVdF: Super-P = 70 : 10 : 20.

A practical liquid carbonate-based electrolyte was used as a base electrolyte, the composition of which was 1 M $LiPF_6$ in a mixture of ethylene carbonate (EC) and ethyl methyl carbonate (EMC) at 1 : 2 in volume. 2 wt. % of Pyrd-PVA-CN was dissolved in the base liquid electrolyte for organogel electrolytes. All electrolytes were made in a glove box (Mbraun) under controlled atmosphere at <0.1 ppm O_2 and H_2O. The cells containing the Pyrd-PVA-CN-present electrolyte were allowed to wet for 12 h for wetting. Thereafter, they were charged and discharged at 0.1 C for the solid-electrolyte interphase (SEI) layer formation. Then, the cells were stored at 60 ^oC for 3 h for the *in situ* gelation of Pyrd-PVA-CN.

Electrochemical characterization

Galvanostatic potential profiles, cyclic voltammograms, linear sweep voltammograms and impedance spectra were obtained by using a battery tester (WonATech, WBCS 3000) or a potentiostat (Biologic, VSP300). A conductivity meter (Mettler-Toledo, SevenMulti with an InLab 710 platinum 4-pole conductivity probe) was used for measuring ionic conductivities of electrolytes.

Lithium ion transference numbers (t_{Li+}) of electrolytes were potentiostatically estimated.[2] Electrolytes of interest were introduced to symmetric cells of lithium metals (Li||Li) with a separator. The Pyrd-PVA-CN-containing liquid electrolyte was gelated at the same condition used for other electrochemical tests after wetting for 12 h. The initial (i^0) and the steady-state (i^s) currents of a Li||Li cell were measured under a polarization potential at 10 mV. Impedance spectra (10 mHz to 200 kHz) were obtained before (R_i^0) and after (R_i^s) the potentiostatic polarization. The t_{Li+} was calculated as following equation;

$$t_{Li} += \frac{i^s(\Delta V - i^0 R_i^0)}{i^0(\Delta V - i^s R_i^s)}$$

A quartz crystal microbalance (QCM; SEIKO QCM922) was used for measuring the change in the amount of Mn^{2+} chelation on PVA-CN or Pyrd-PVA-CN. 20 μg of 5 wt. % polymer in the same electrolyte used for LIB cells was dropped on gold-coated quartz crystal resonators (0.196 cm^2) and then thermally gelated at 60 ^oC. Resonance frequencies were measured along time in the absence and presence of 2,000 ppm Mn^{2+} in the same electrolyte except of 1 M $LiClO_4$ instead of $LiPF_6$.

Structural and physicochemical characterization

Pyrd-PVA-CN was spectroscopically identified by nuclear magnetic resonance spectroscopy (H^1-NMR with d_6-DMSO as a NMR solvent; Bruker Avance 300) and infrared spectroscopy (FTIR; Bruker ALPHA). Cathode samples were crystallographically identified by a X-ray diffraction (XRD) spectrometer (Rigaku D/MAX2500V/PC) with Cu-Kα radiation. The amounts of Mn metal deposited on anodes were measured by an optical emission spectrometer with samples atomized by inductively coupled plasma (ICP-OES; Perkin Elmer ELAN DRC-II).

MnF_2 on cathode as well as Mn metal on anode was identified by secondary ion mass spectra of cathode samples with time-of-flight mass analysis (TOF-SIMS; IONTOF TOF.SIMS 5). Oxidation states of Mn of LMO cathodes were investigated by electron energy loss spectroscopy of a scanning transmission electron microscopy (STEM-EELS; JEM-2100F HR-TEM).

Density functional theory calculation

Dmol[3] program was used for spin-polarized density functional theory (DFT) calculations.[3, 4] The generalized gradient approximation (GGA) with Perdew-Burcke-Ernzerhof (PBE) functional[5] was employed for the exchange correlation potential. The DNP 4.4 basis set was used with a global orbital cutoff of 4.7 Å. The core electrons were explicitly treated as all electrons with relativistic effect. The long-range van der Waals interactions were corrected by Grimme's method.[6] The self-consistent field calculation was performed with a thermal smearing of 0.005 Ha until convergence criterion of 1×10^{-6} Ha was satisfied. The convergence criteria for geometry optimization were set to 1×10^{-5} Ha for energy change, 0.002 $Å^{-1}$ for the maximum force, 0.005 for the maximum displacement, respectively. Solvent environments were described by a conductor-like screening model (COSMO)[7] with dielectric constants (ε) of 46.7 and 24.82 for DMSO and EC/EMC (1:2 v/v), respectively. Dielectric constant of EC/EMC was calculated by the quadratic mixing rule.[8] The atomic charge was estimated by the Mulliken population analysis.[9] The Gibbs free energies of formation ($\Delta_f G$) of Mn^{2+} complexes were estimated by calculating the change in Gibbs free energy during the complexation of Mn^{2+} with functional groups of PVA-CN and/or solvent molecules in solvent environment at 298.15 K:

$$\Delta_f G = \Delta_f H - T\Delta_f S = \Delta_f E + P\Delta_f V - T\Delta_f S \approx \Delta_f E - T\Delta_f S$$

where H = enthalpy; S = entropy; E = energy; and V = volume. Here, $P\Delta_f V$ term was ignored since the complexation occurs in solution states where pressure effect is negligible with a marginal change of volume. E was calculated by considering the contributions of translational, rotational and vibrational motions:

$$E = E_0 + E_{\text{translation}} + E_{\text{rotation}} + E_{\text{vibration}};\ S = S_{\text{translation}} + S_{\text{rotation}} + S_{\text{vibration}}$$

where E_0 is the electronic energy of ground state. Translational, rotational and vibrational motions of Mn^{2+} were neglected. Two different solvent environments were considered for the Mn^{2+} complexation: EC/EMC at 1:2 v/v (ε = 24.82) used for LIB tests and DMSO (ε = 46.7) used for NMR spectroscopy:

$$Mn^{2+}\ (sol) + n\ EC\ (sol) \rightarrow Mn^{2+}(EC)_n\ (sol)$$

$$Mn^{2+}\ (sol) + n\ EMC\ (sol) \rightarrow Mn^{2+}(EMC)_n\ (sol)$$

$$Mn^{2+}\ (sol) + Pyrd\ (sol) + n\ EC\ (sol) \rightarrow Mn^{2+}(Pyrd)(EC)_n\ (sol)$$

$$Mn^{2+}\ (sol) + Pyrd\ (sol) + n\ EMC\ (sol) \rightarrow Mn^{2+}(Pyrd)(EMC)_n\ (sol)$$

$$Mn^{2+}\ (sol) + Pyrd\ (sol) + n\ DMSO\ (sol) \rightarrow Mn^{2+}(Pyrd)(DMSO)_n\ (sol).$$

References

1. B. Neises and W. Steglich, *Angew. Chem. Int. Ed.*, 1978, **17**, 522-524.
2. S. Zugmann, M. Fleischmann, M. Amereller, R. M. Gschwind, H. D. Wiemhöfer and H. J. Gores, *Electrochim. Acta*, 2011, **56**, 3926-3933.
3. B. Delley, *J. Chem. Phys.*, 2000, **113**, 7756-7764.
4. B. Delley, *J. Chem. Phys.*, 1990, **92**, 508-517.
5. J. P. Perdew, K. Burke and M. Ernzerhof, *Phys. Rev. Lett.*, 1996, **77**, 3865.
6. S. Grimme, *J. Comput. Chem.*, 2006, **27**, 1787-1799.
7. A. Klamt and G. Schüürmann, *J. Chem. Soc., Perkin Trans. 2*, 1993, 799-805.
8. D. S. Hall, J. Self and J. Dahn, *J. Phys. Chem. C*, 2015, **119**, 22322-22330.
9. R. S. Mulliken, *J. Chem. Phys.*, 1955, **23**, 1833-1840.

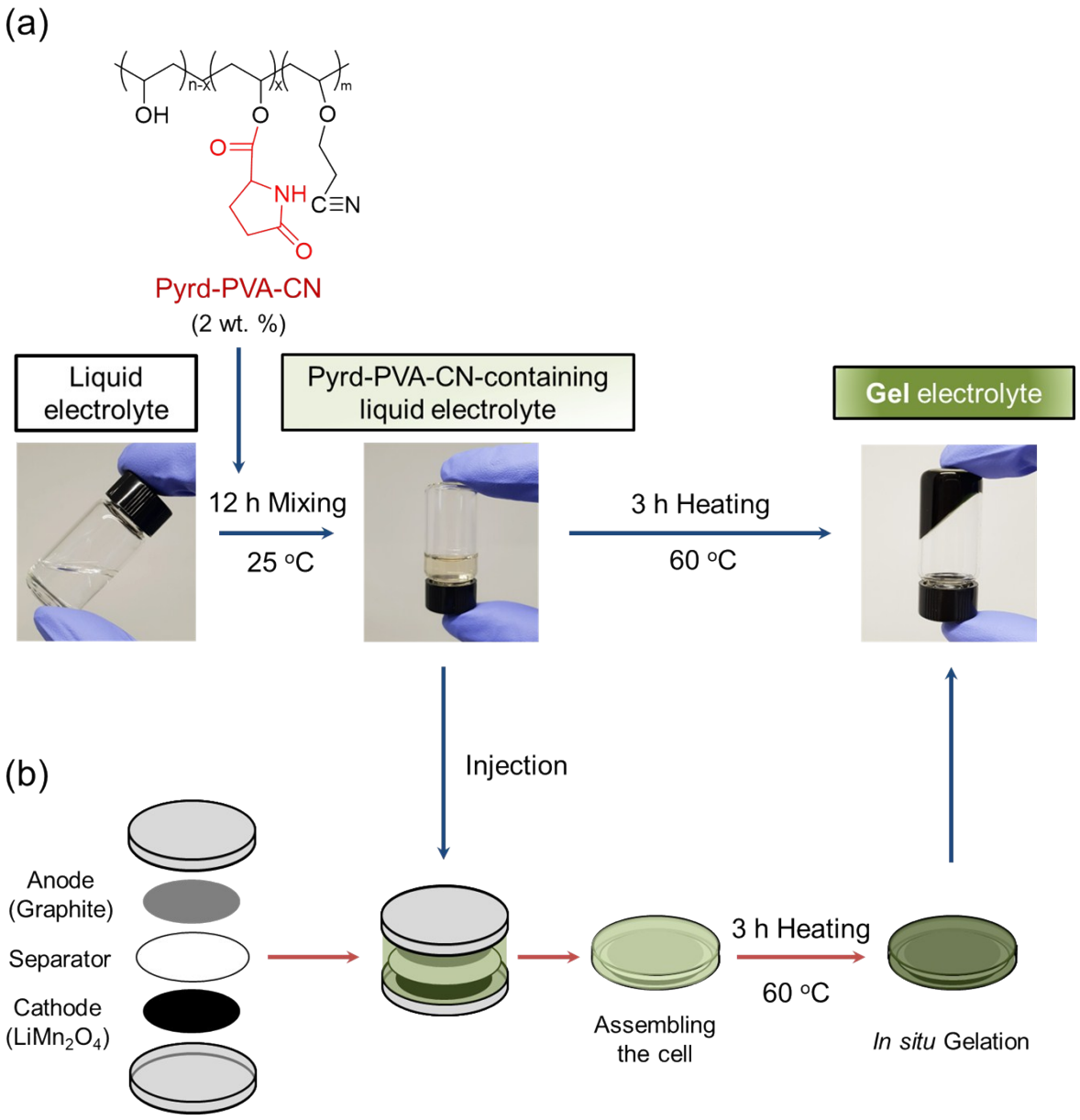

Figure S1. *In situ* gelation of Pyrd-PVA-CN in a vial (a) and a coin cell of LMO||graphite (b).

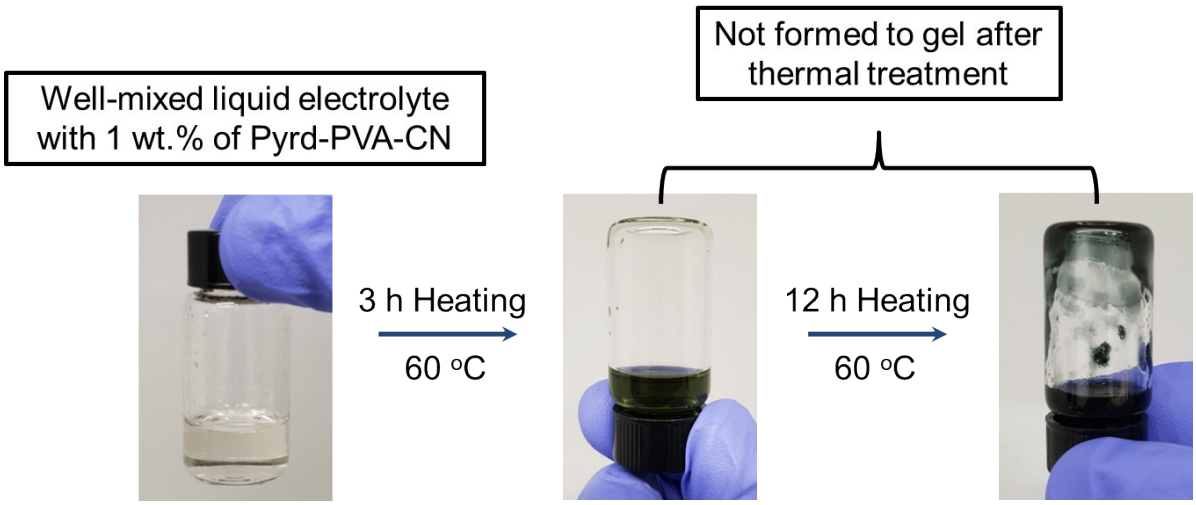

Figure S2. Failed gelation of the liquid electrolyte containing 1wt. % Pyrd-PVA-CN at 60 °C for 15 h.

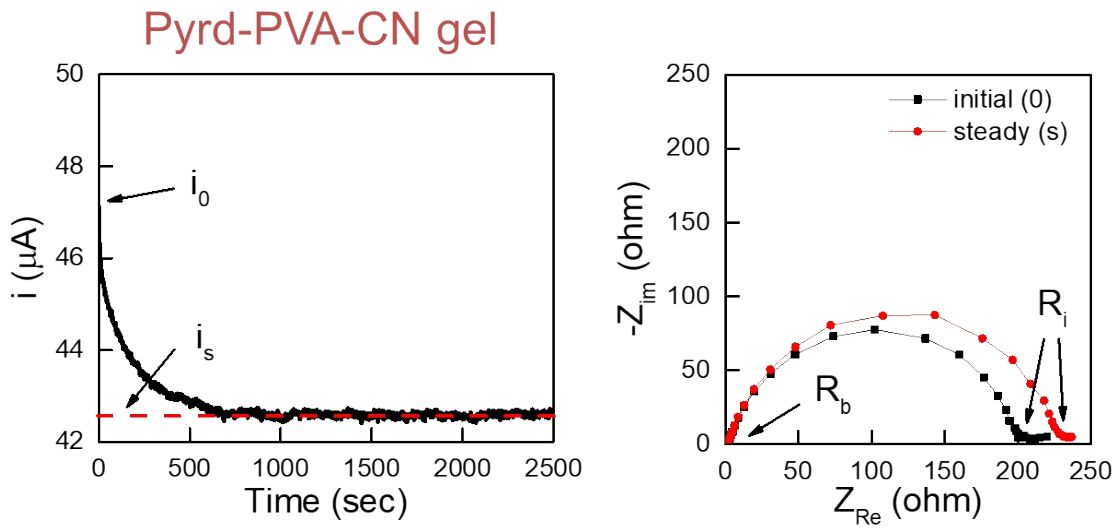

	i^0 (uA)	i^s(uA)	R_b^0 (ohm)	R_b^s(ohm)	R_i^0(ohm)	R_i^s(ohm)	ΔV(V)
Gel	47.12	42.56	2.42	2.23	199.3	227.7	0.01

$$t_+ = \frac{i^s(\Delta V - i^0 R_i^0)}{i^0(\Delta V - i^s R_i^s)} = 0.87$$

Figure S3. Measuring lithium ion transference number (t_+) of Pyrd-PVA-CN gel by a potentiostatic polarization method.

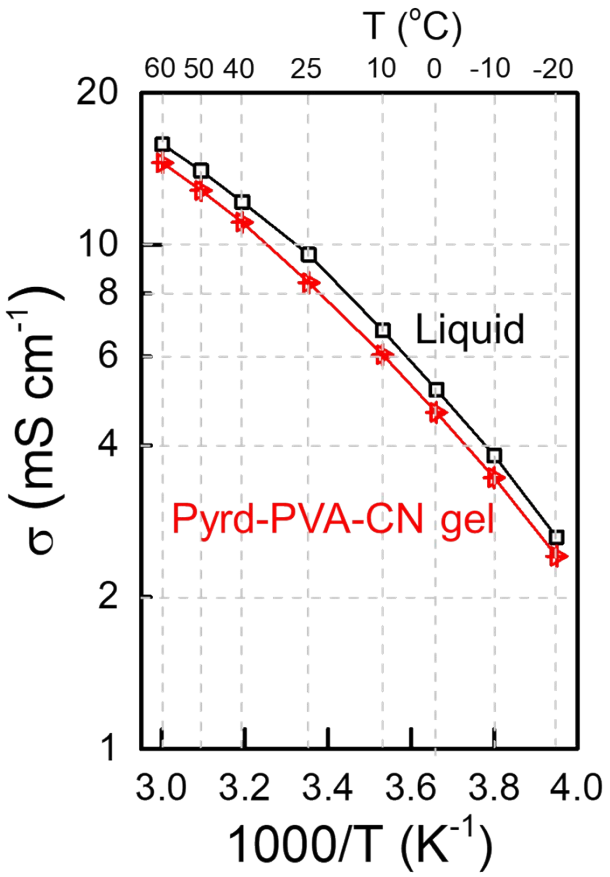

Figure S4. Ionic conductivities (σ) of the carbonate-based liquid electrolyte of 1 M $LiPF_6$ in EC: EMC at 1 : 2 in volume and the gel electrolyte of 2 wt. % Pyrd-PVA-CN in the same liquid electrolyte from -20 °C to 60 °C. The temperature on the abscissa is the temperature of the conductivity measurement. A conductivity probe (Mettler-Toledo, InLab 710 platinum 4-pole conductivity probe) was immersed in the liquid electrolyte which Pyrd-PVA-CN was dissolved in. Then, the polymer-containing solution was heated at 60 °C for 3 h for gelation. Then the conductivities of the organogel were measured at various temperatures.

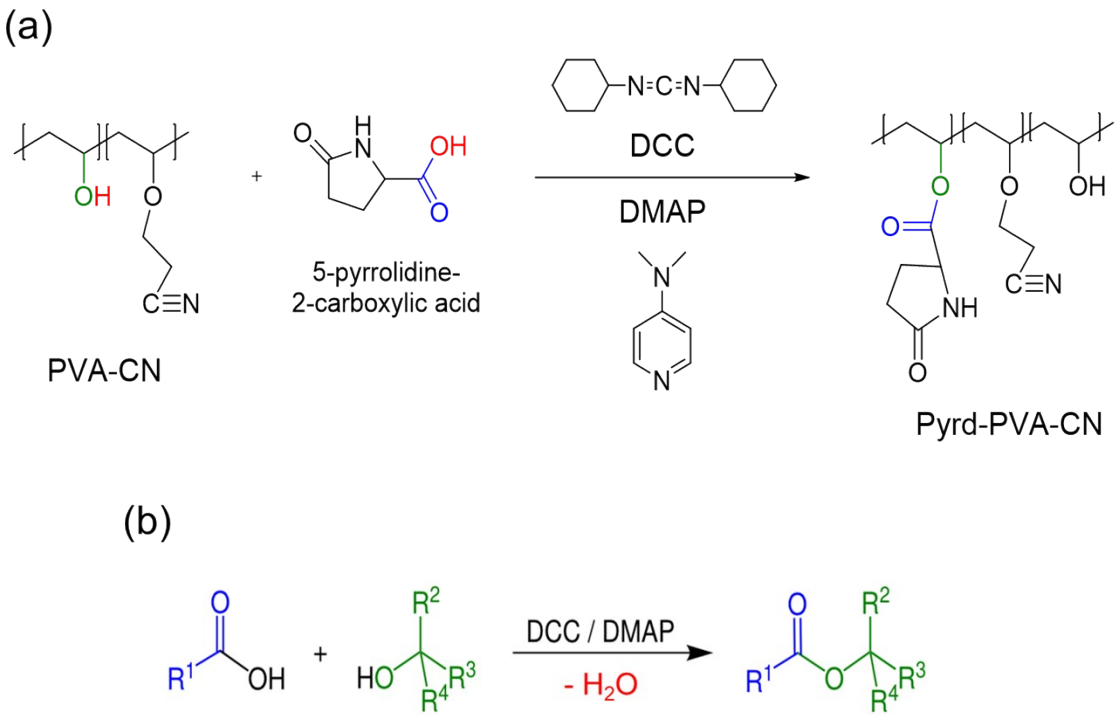

Figure S5. Pyrd-PVA-CN. (a) Synthesis reaction. (b) Steglich esterification reaction.

DCC = N,N'-Dicyclohexylcarbodiimide; DMAP = Dimethylaminopyridine.

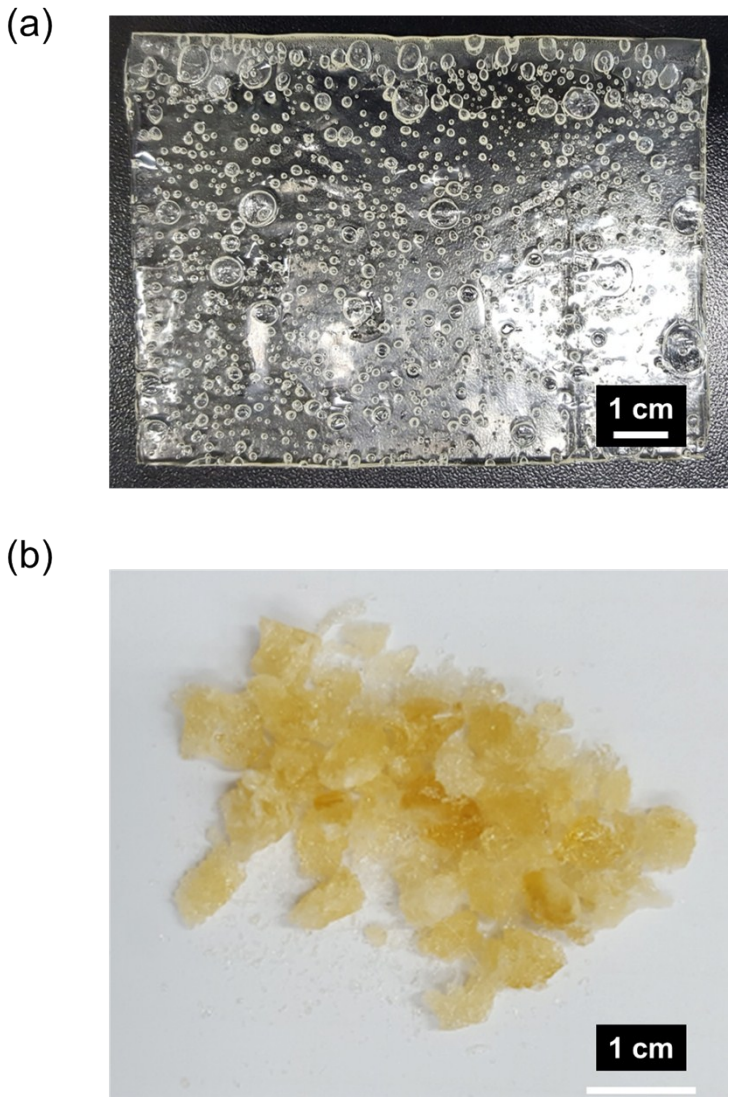

Figure S6. Macroscopic appearance of gel polymers by photos. (a) PVA-CN and (b) Pyrd-PVA-CN

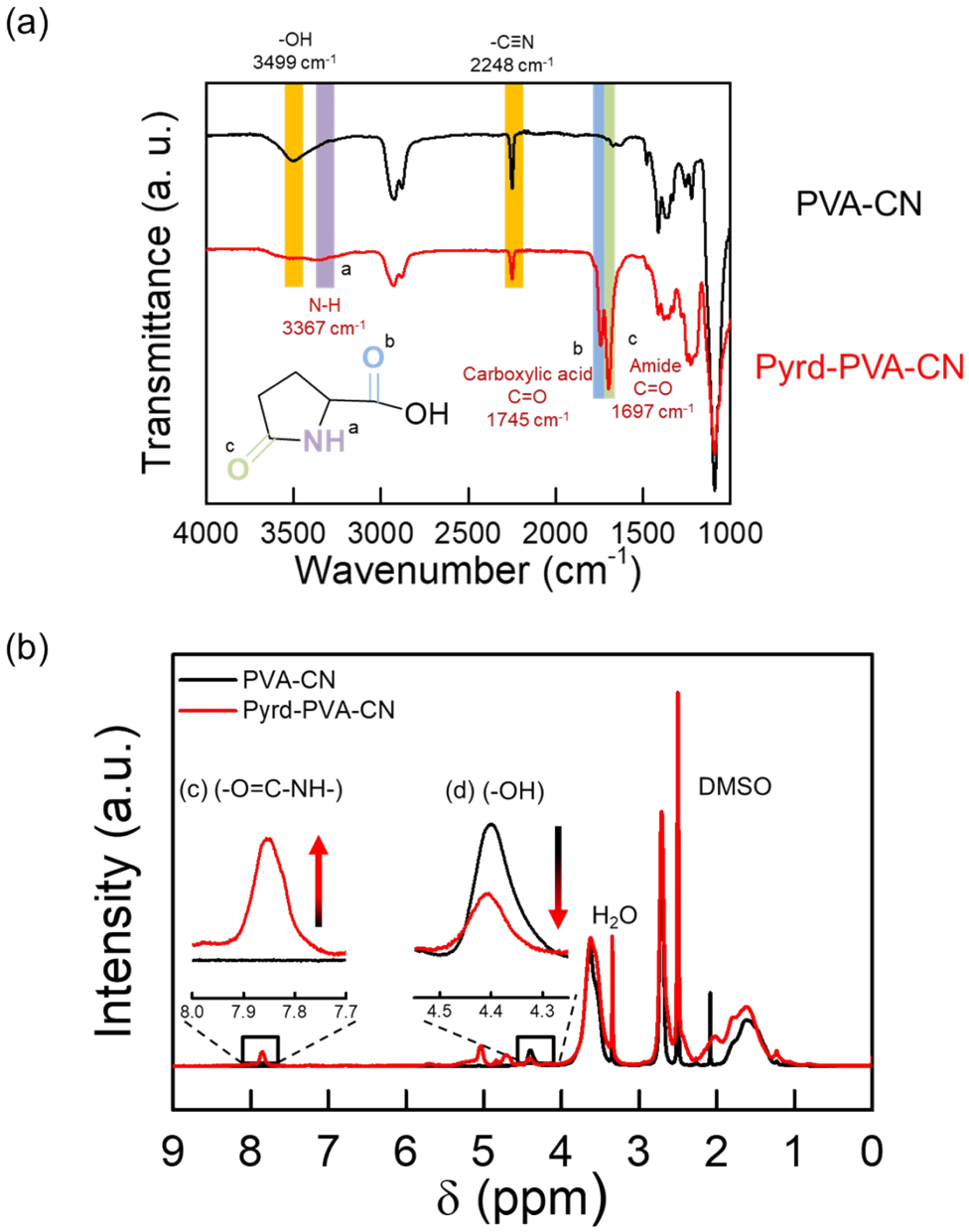

Figure S7. Synthesis confirmation. (a) Fourier transform infrared (FTIR) spectra of PVA-CN and Pyrd-PVA-CN. PVA-CN (before synthesis) has a sharp peak at 2248 cm^{-1} belonging to C≡N and a peak for alcohol (-OH) at 3499 cm^{-1}. Pyrd-PVA-CN (after synthesis) had new peaks such as a broad and small peak at 3367 cm^{-1} belonging to N-H with two different C=O peaks at 1697 cm^{-1} and 1745 cm^{-1} for amide and carboxylic acid group, respectively. (b) ^{1}H NMR spectra of PVA-CN (black) and Pyrd-PVA-CN (red). Inset: magnified region (c) amide group and (d) alcohol group.

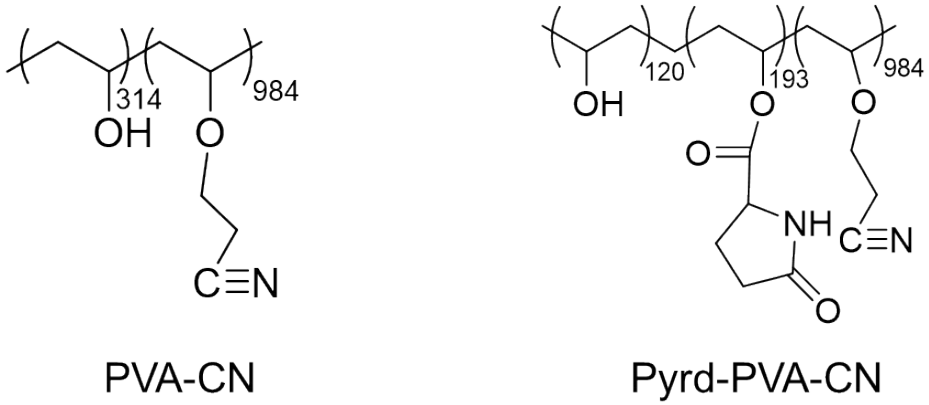

PVA-CN Pyrd-PVA-CN

Figure S8. Estimated numbers of repeating units for PVA-CN and Pyrd-PVA-CN.

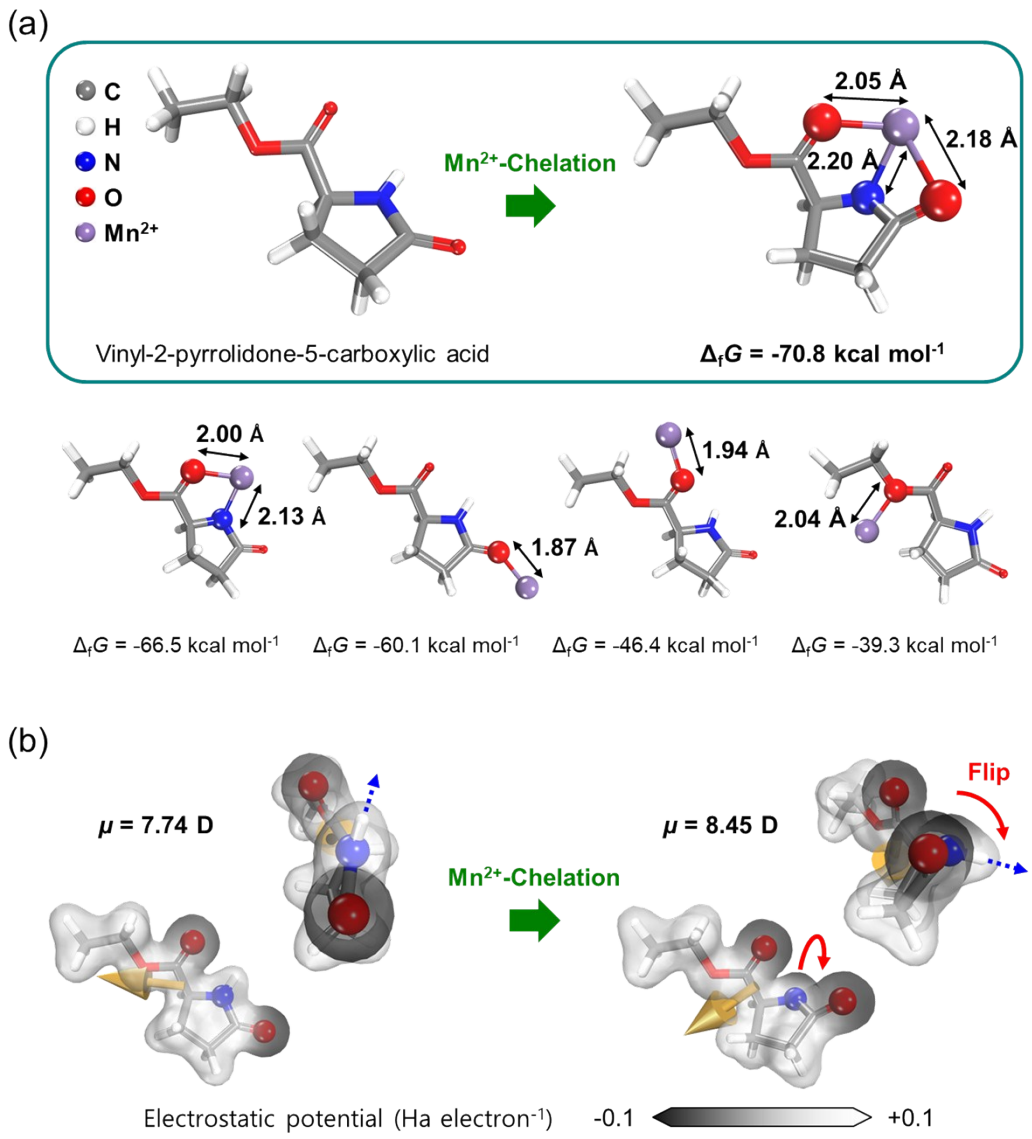

Figure S9. Vinyl-2-pyrrolidone-5-carboxylic acid as a model of pyrrolidone (Pyrd) of Pyrd-PVA-CN and various Mn^{2+}(Pyrd) complexes in EC/EMC at 1:2 v/v (ε = 24.82). Solvent molecules were not allowed to coordinate to Mn^{2+}. (a) Optimized geometries with Gibbs free energy of formation ($\Delta_f G$). The lowest $\Delta_f G$ (-70.8 kcal mol^{-1}) was achieved by the triply coordinated complex of Mn^{2+}-Pyrd in the absence of solvent molecules. In the presence of solvent, Mn^{2+} was double-coordinated to Pyrd at the optimized conformation. (b) Electrostatic potential maps with electric dipole moments (μ) of the pyrrolidone group before and after Mn^{2+} chelation. The electrostatic potential was mapped on the isosurface of electron density with the isovalue of 0.2 e $Å^{-3}$.

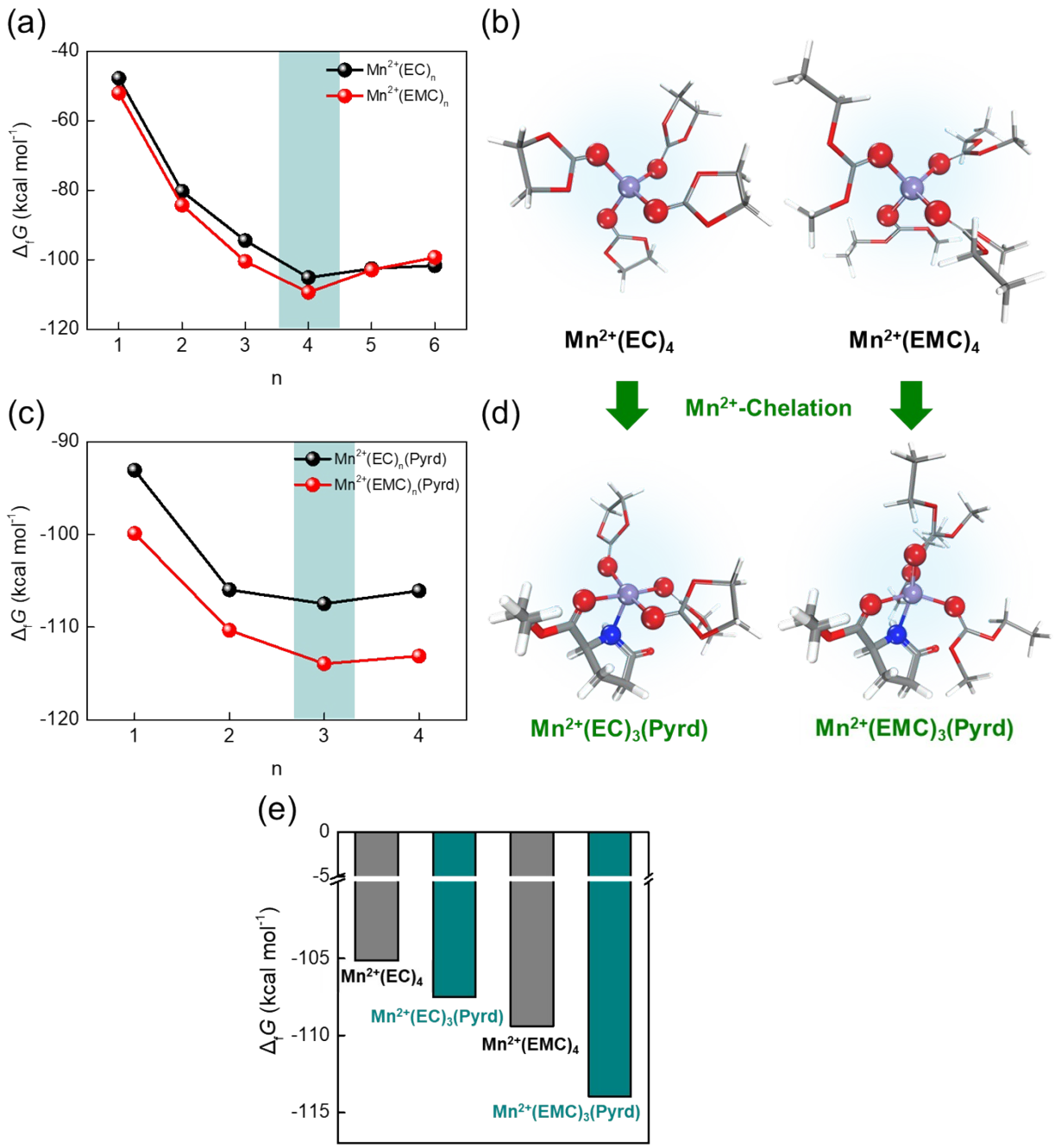

Figure S10. Mn^{2+} complex formation in EC/EMC at 1 : 2 in volume in the absence (a and b) and the presence of pyrrolidone groups (c and d). Solvent molecules were allowed to coordinate to Mn^{2+} or solvate Mn^{2+}. EC = ethylene carbonate; EMC = ethyl methyl carbonate. (a and c) Gibbs free energies of formation ($\Delta_f G$) of Mn^{2+} complexes. (b and d) Optimized geometries. (e) $\Delta_f G$ comparison.

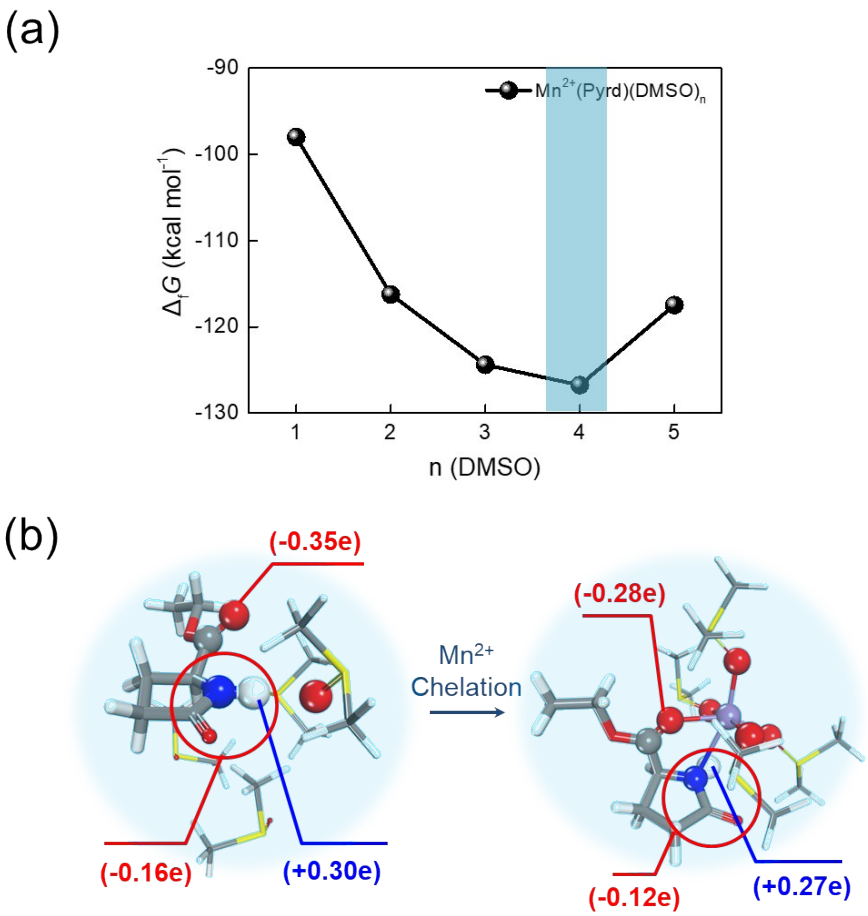

Figure S11. (a) Gibbs free energy of formation ($\Delta_f G$) of Mn^{2+}(Pyrd)(DMSO)$_n$ complexes in DMSO solvent. Mn^{2+}(Pyrd)(DMSO)$_n$ complex was considered to the most stable structure. (b) Optimized geometries of (Pyrd)(DMSO)$_4$ and Mn^{2+}(Pyrd)(DMSO)$_4$ complexes. The values given in the parentheses represent Mulliken charge of -COO- and -CONH- groups (red color), and H atom in pyrrolidone group (blue color).

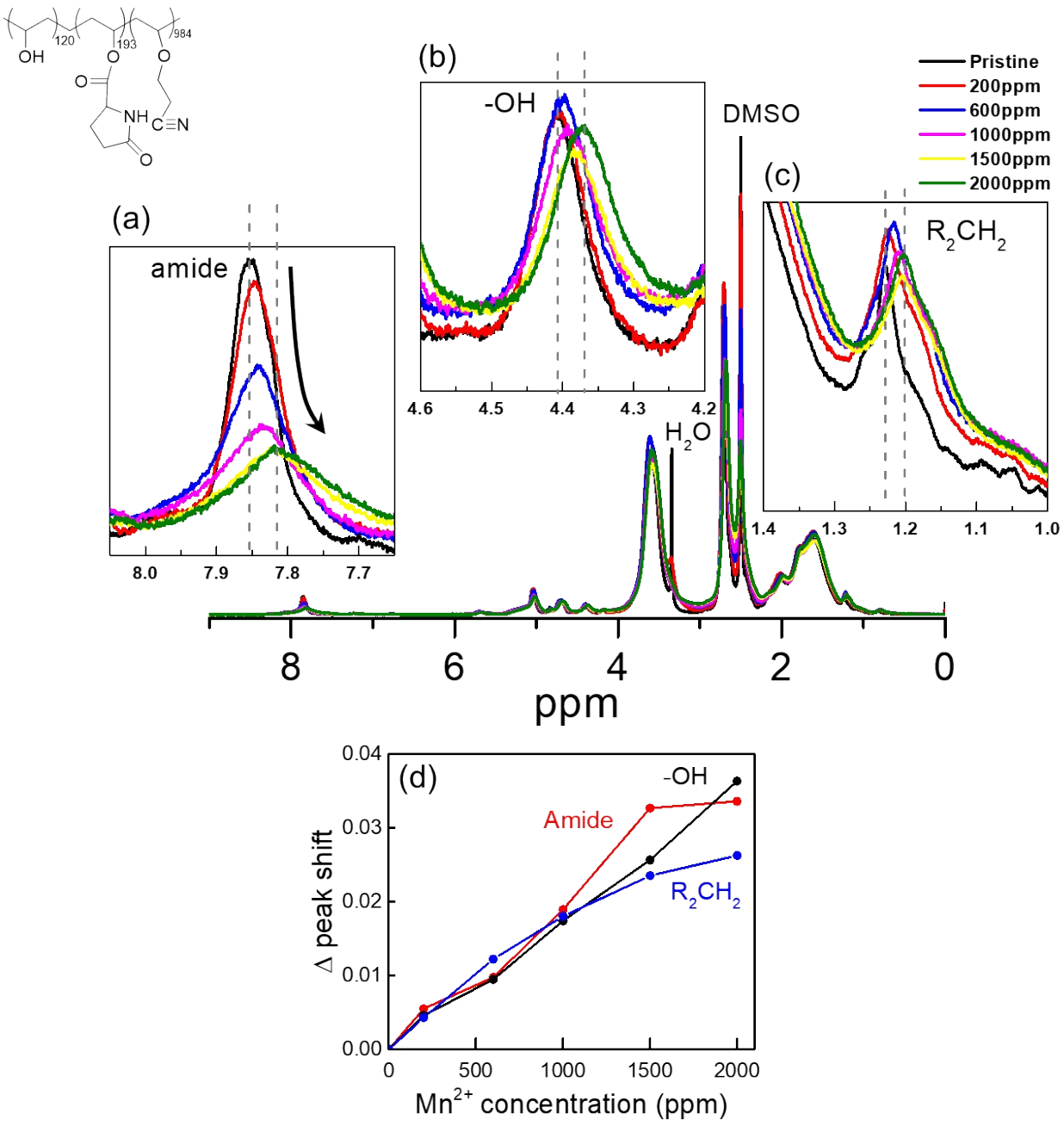

Figure S12. ^{1}H NMR spectra of Pyrd-PVA-CN in the presence of Mn^{2+}. Pyrd-PVA-CN and $Mn(ClO_4)_2$ were dissolved in DMSO-d_6 for the NMR measurements. (a) The peaks assigned to proton of the amide group of pyrrolidone at 7.84 ppm. (b) The peaks assigned to proton of the alcohol group attached to polymer backbone at 4.4 ppm. (c) The peaks assigned to the aliphatic protons at 1.6 ppm. (d) Peak shifts in the peaks of ^{1}H NMR of Pyrd-PVA-CN with Mn^{2+} concentration from 0 ppm Mn^{2+} to 2000 ppm Mn^{2+}.

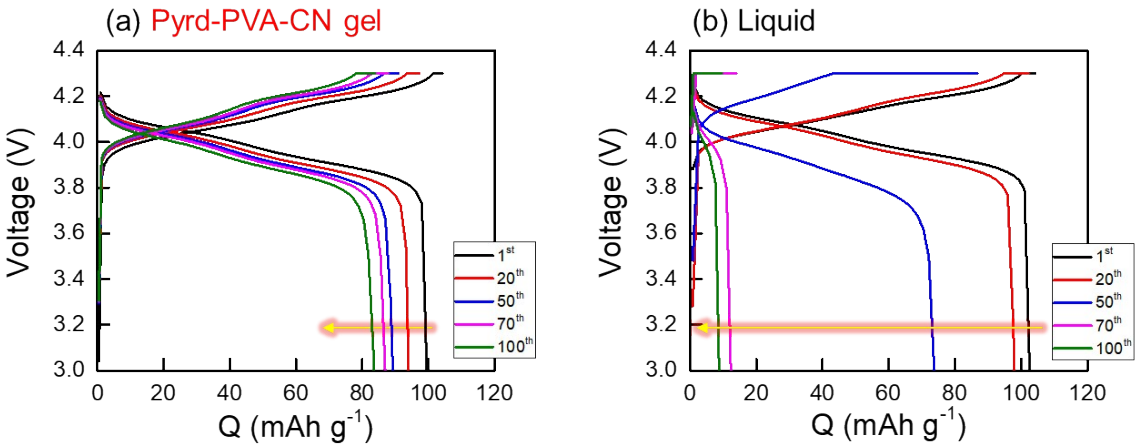

Figure S13. Cell voltage profiles of Figure 2a. (a) Pyrd-PVA-CN gel electrolyte. (b) Liquid electrolyte.

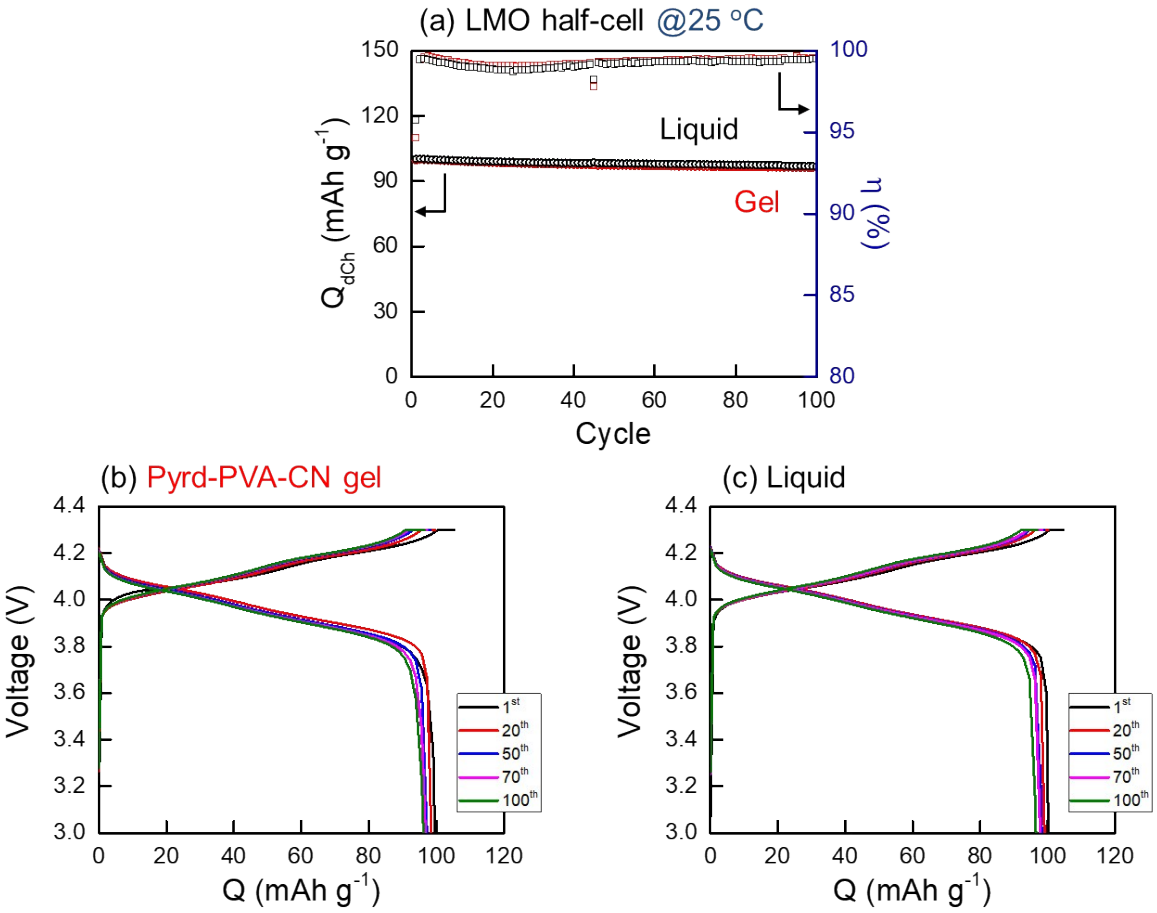

Figure S14. LMO half cells using only the 4 V reaction at the room temperature. (a) Cyclability at 1C charge followed by 1C discharge. (b and c) Cell voltage profiles in the presence of Pyrd-PVA-CN gel electrolyte (b) and the corresponding liquid electrolyte (c).

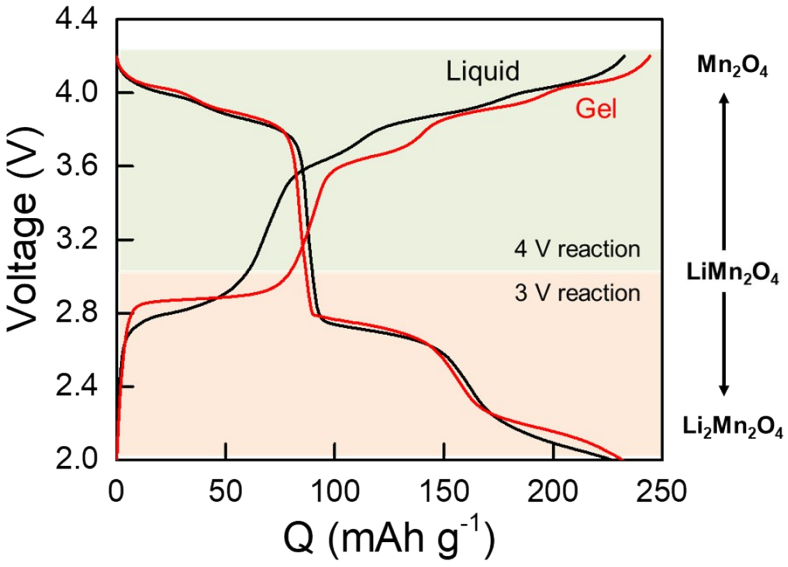

Figure S15. Galvanostatic charge/discharge potential profile both the cell based on Liquid and Gel at the first cycle. The discharge capacity was obtained of 227 mAh g^{-1} for Liquid and 232 mAh g^{-1} for Gel, respectively. 1 M $LiPF_6$ in mixture of ethylene carbonate (EC) and ethyl methyl carbonate (EMC) (1:2 v/v) as a Liquid and gelated electrolyte by injected 2 wt. % Pyrd-PVA-CN as a Gel were used.

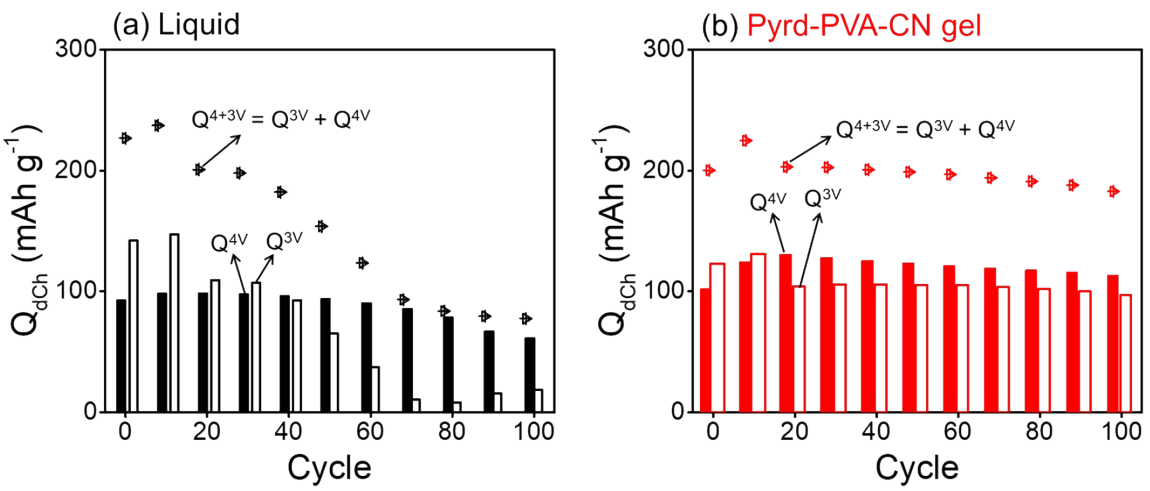

Figure S16. Capacities of 4 V reaction (Q^{4V}, solid bar on the left) and 3 V reaction (Q^{3V}, open bar on the right) in Liquid (a) and Gel (b)

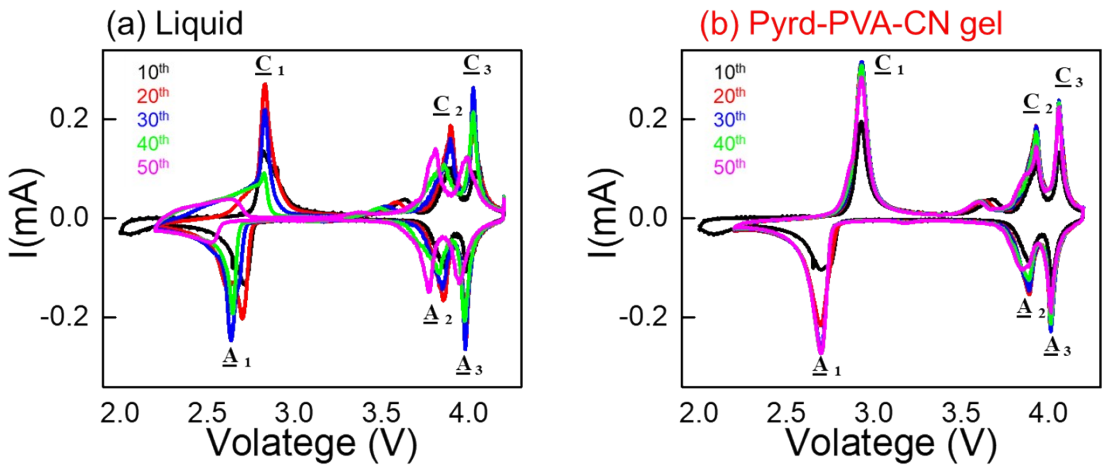

Figure S17. **Cyclic voltammograms in the liquid electrolyte (a) and the Pyrd-PVA-CN gel electrolyte (b).** Scan rate = 0.06 mV s^{-1} for the initial 10 cycles followed by 0.1 mV s^{-1} after the 10^{th} cycle. Cathodic and anodic peaks were indicated by C and A, respectively. C_1 and A_1 are for the 3 V reaction while the other peaks are for the 4 V reaction.

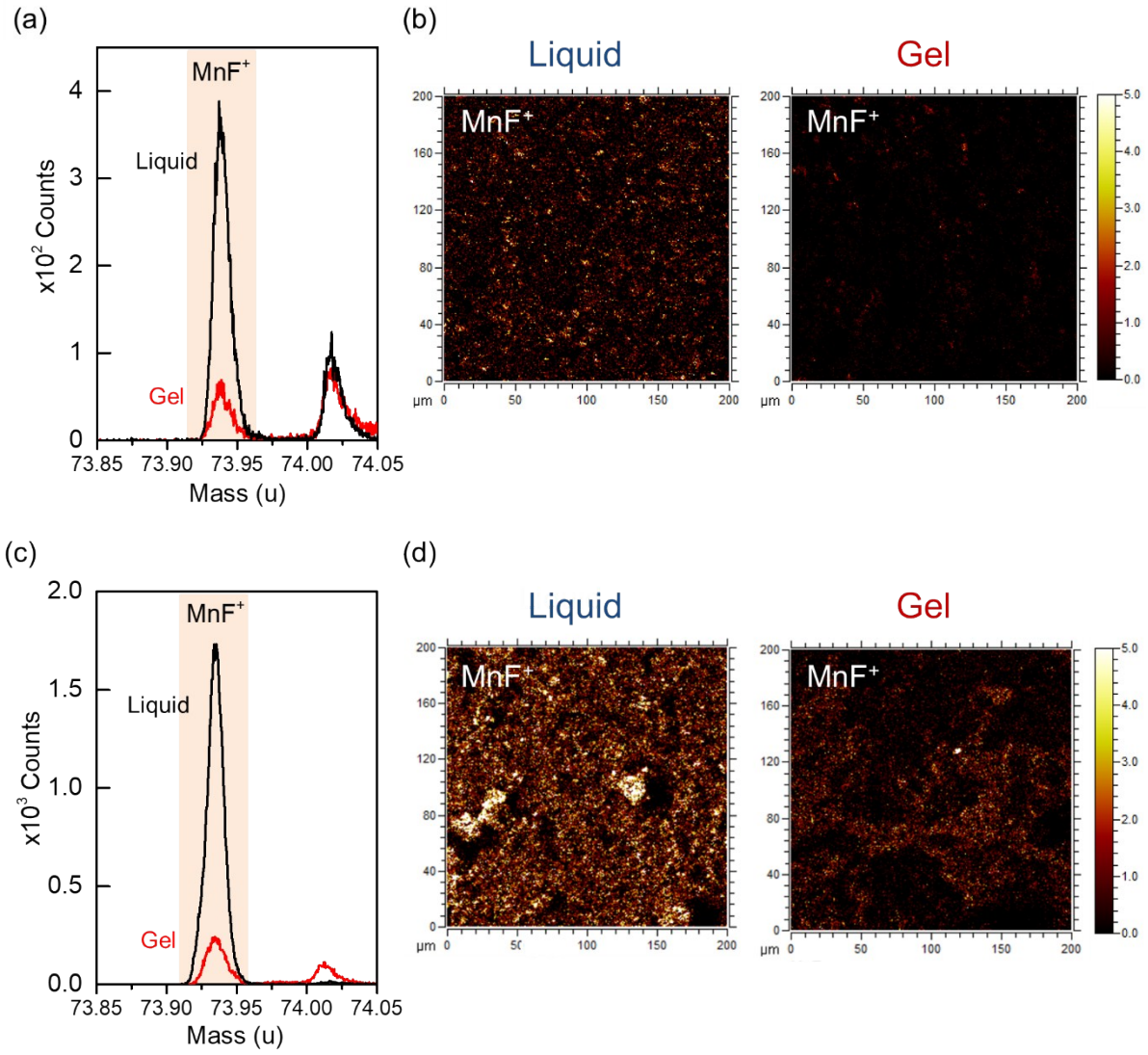

Figure S18. MnF_2 formed on the surface of LMO cathodes obtained from (a and b) LMO||Li cells experiencing 100 cycles (the same condition used in **Figure 2a**) and (c and d) LMO||graphite cells after 100 cycles (the same condition used in **Figure 2b**) (a and c) Mass spectra of MnF^+ and (b and d) 2D maps by TOF-SIMS.

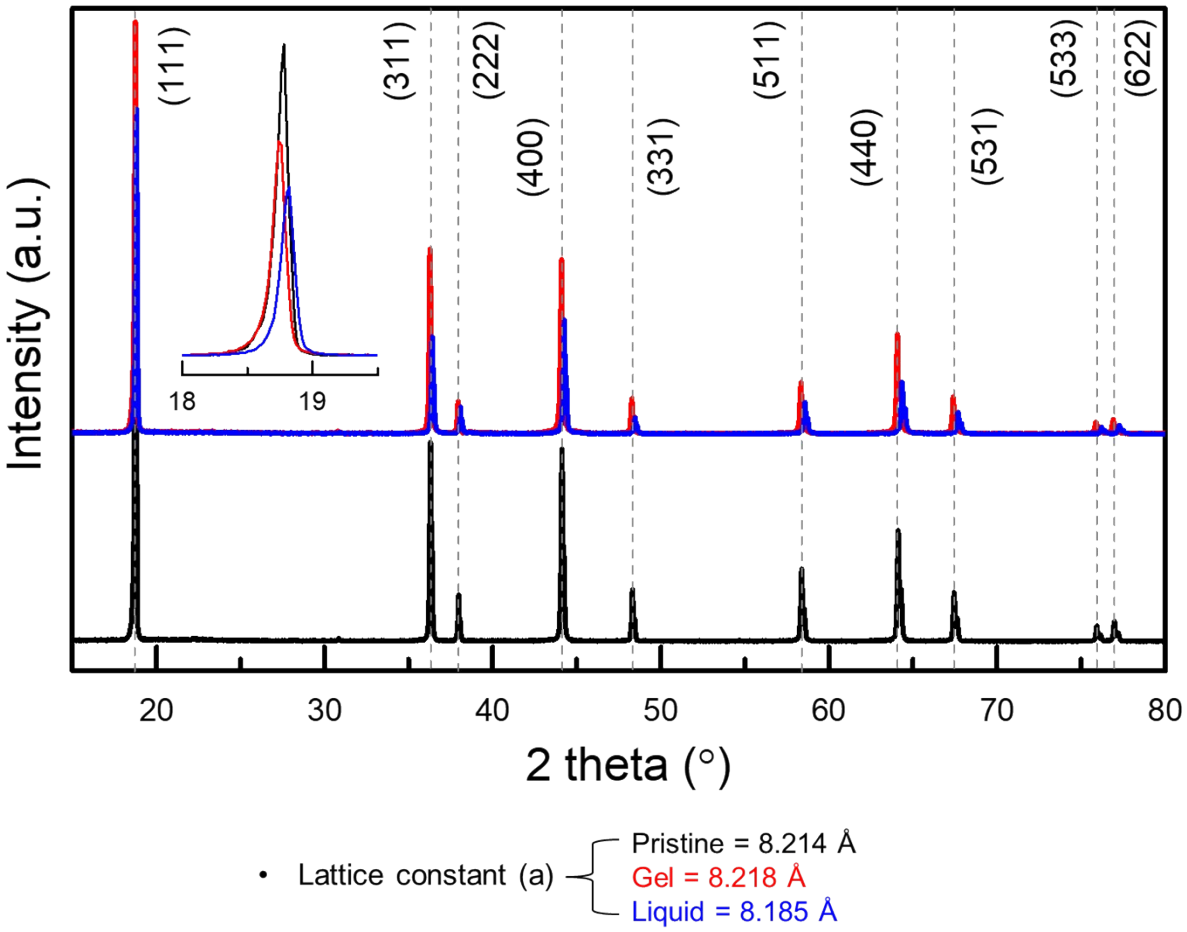

Figure S19. XRD patterns of LMOs: black = pristine LMO; blue = LMO experiencing 100 cycles at 55 °C in the liquid electrolyte; red = LMO experiencing the same cycles in Pyrd-PVA-CN gel.

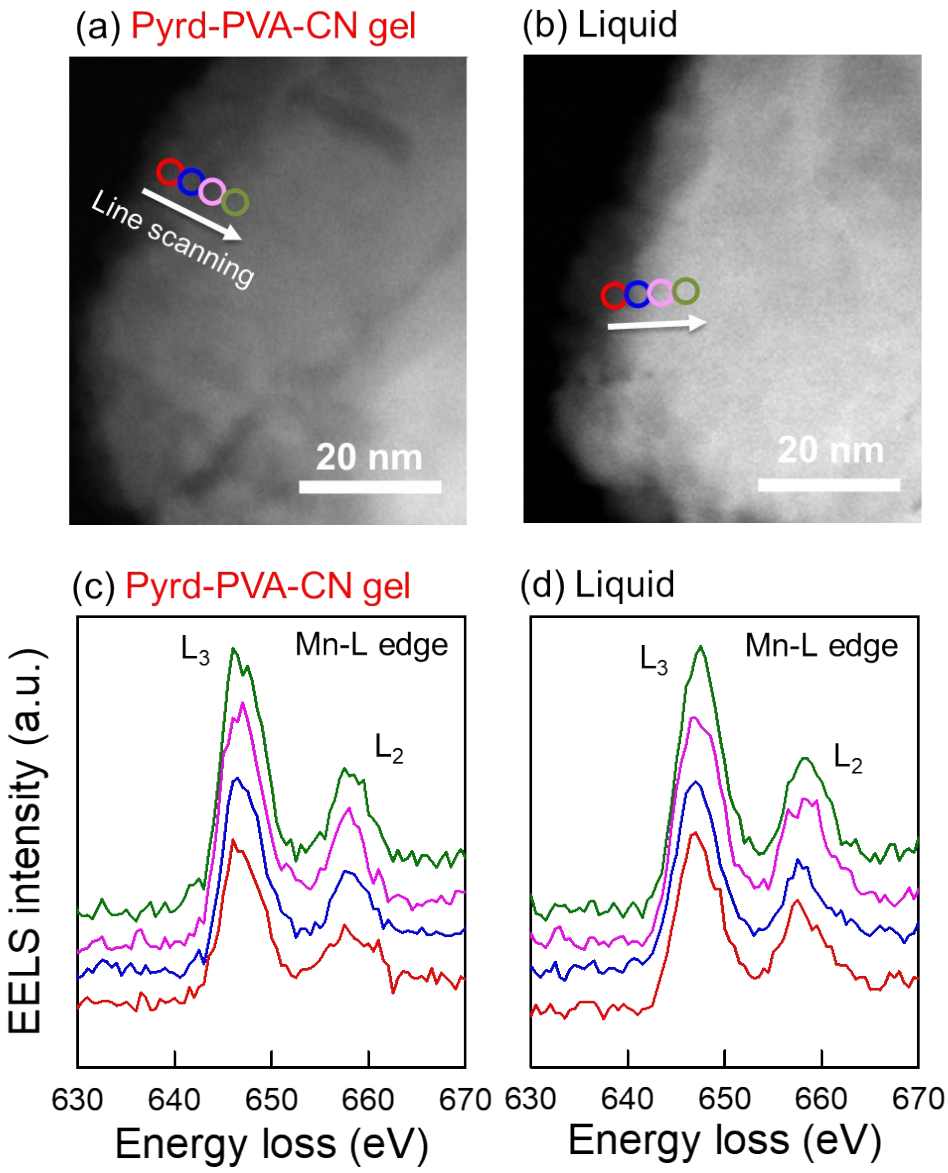

Figure S20. (a and b) Scanning transmission electron microscopy (STEM) images of LMO particles experiencing 100 cycles. (c and d) Electron energy loss spectra (EELS) of Mn-L edge of LMO obtained from the indicated spots of the STEM images in a and b. The images and spectra were obtained in the liquid electrolyte (a and c) and in the Pyrd-PVA-CN gel electrolyte (b and d).